Experimental demonstration of a multi-wavelength distributed feedback semiconductor laser array with an equivalent chirped grating profile based on the equivalent chirp technology

Wangzhe Li[1], Xia Zhang[2], and Jianping Yao[1,*]

[1]*Microwave Photonics Research Laboratory, School of Electrical Engineering and Computer Science, University of Ottawa, Ottawa, ON K1N 6N5, Canada*
[2]*CMC Microsystems, Kingston, ON K7L 3N6, Canada*
[*] *jpyao@eecs.uOttawa.ca*

Abstract: We report, to the best of our knowledge, the first realization of a multi-wavelength distributed feedback (DFB) semiconductor laser array with an equivalent chirped grating profile based on equivalent chirp technology. All the lasers in the laser array have an identical grating period with an equivalent chirped grating structure, which are realized by nonuniform sampling of the gratings. Different wavelengths are achieved by changing the sampling functions. A multi-wavelength DFB semiconductor laser array is fabricated and the lasing performance is evaluated. The results show that the equivalent chirp technology is an effective solution for monolithic integration of a multi-wavelength laser array with potential for large volume fabrication.

OCIS codes: (060.2330) Fiber optics communications; (140.3490) Lasers, distributed-feedback; (250.5300) Photonic integrated circuits.

References and links

1. K. Lawniczuk, M. Wale, P. Szczepanski, R. Piramidowicz, M. Smit, and X. Leijtens, "Photonic multiwavelength transmitters with DBR laser array for optical access networks," in Optical Fiber Communication Conference/National Fiber Optic Engineers Conference 2013, paper JW2A.35.
2. L. Razzari, D. Duchesne, M. Ferrera, R. Morandotti, S. Chu, B. E. Little, and D. J. Moss, "CMOS-compatible integrated optical hyper-parametric oscillator," Nat. Photonics **4**(1), 41–45 (2010).
3. S. W. Ryu, S. B. Kim, J. S. Sim, and J. Kim, "Monolithic integration of a multiwavelength laser array associated with asymmetric sampled grating lasers," IEEE J. Sel. Top. Quantum Electron. **8**(6), 1358–1365 (2002).
4. J. Van Campenhout, L. Liu, P. R. Romeo, D. Van Thourhout, C. Seassal, P. Regreny, L. Di Cioccio, J.-M. Fedeli, and R. Baets, "A compact SOI-integrated multiwavelength laser source based on cascaded InP microdisks," IEEE Photon. Technol. Lett. **20**(16), 1345–1347 (2008).
5. V. Karagodsky, B. Pesala, C. Chase, W. Hofmann, F. Koyama, and C. J. Chang-Hasnain, "Monolithically integrated multi-wavelength VCSEL arrays using high-contrast gratings," Opt. Express **18**(2), 694–699 (2010).
6. K. Lawniczuk, C. Kazmierski, J. Provost, M. J. Wale, R. Piramidowicz, P. Szczepanski, M. K. Smit, and X. J. M. Leijtens, "InP-based photonic multiwavelength transmitter with DBR laser array," IEEE Photon. Technol. Lett. **25**(4), 352–354 (2013).
7. J. Carroll, J. Whiteaway, and D. Plumb, Distributed feedback semiconductor lasers, 1998, Inst. Elec. Eng.
8. S. Akiba, M. Usami, and K. Utaka, "1.5 μm λ/4-shifted InGaAsP/InP DFB lasers," J. Lightwave Technol. **5**(11), 1564–1573 (1987).
9. P. Zhou and G. S. Lee, "Mode selection and spatial hole burning suppression of a chirped grating distributed feedback laser," Appl. Phys. Lett. **56**(15), 1400–1402 (1990).
10. P. Zhou and G. S. Lee, "Phase shifted distributed feedback laser with linearly chirped grating for narrow linewidth and high-power operation," Appl. Phys. Lett. **58**(4), 331–333 (1991).
11. H. Hillmer and B. Klepser, "Low-cost edge-emitting DFB laser arrays for DWDM communication systems implemented by bent and titled waveguides," IEEE J. Quantum Electron. **40**(10), 1377–1383 (2004).
12. D. M. Tennant and T. L. Koch, "Fabrication and uniformity issues in λ/4 shifted DFB laser arrays using e-beam generated contact grating masks," Microelectron. Eng. **32**(1–4), 331–350 (1996).
13. Y. Dai and J. P. Yao, "Numerical study of a DFB semiconductor laser and laser array with chirped structure based on the equivalent chirp technology," IEEE J. Quantum Electron. **44**(10), 938–945 (2008).

#192100 - $15.00 USD Received 11 Jun 2013; revised 1 Aug 2013; accepted 1 Aug 2013; published 16 Aug 2013

14. S. Li, Y. Shi, J. Li, R. Gu, X. Tu, and X. Chen, “Experimental demonstration of the corrugation pitch modulated DFB semiconductor laser based on the reconstruction-equivalent-chirp technology,” Proc. Commun. Photon. Conf. 112–113 (2010).
15. Y. Shi, X. Chen, Y. Zhou, S. Li, L. Li, and Y. Feng, “Experimental demonstration of the three phase shifted DFB semiconductor laser based on reconstruction-equivalent-chirp technique,” Opt. Express **20**(16), 17374–17379 (2012).
16. Y. Shi, X. Chen, Y. Zhou, S. Li, L. Lu, R. Liu, and Y. Feng, “Experimental demonstration of eight-wavelength distributed feedback semiconductor laser array using equivalent phase shift,” Opt. Lett. **37**(16), 3315–3317 (2012).
17. J. Li, Y. Cheng, Z. Yin, L. Jia, X. Chen, S. Liu, S. Li, and Y. Lu, “A multiexposure technology for sampled Bragg gratings and its applications in dual-wavelength lasing generation and OCDMA en/decoding,” IEEE Photon. Technol. Lett. **21**(21), 1639–1641 (2009).
18. J. P. Yao, “Microwave photonics,” J. Lightwave Technol. **27**(3), 314–335 (2009).

1. Introduction

High-performance, low-cost semiconductor multi-wavelength lasers (MWLs) have been intensively studied in monolithically integrated optoelectronic field for their significant applications in high-bit-rate long-haul optical fiber communications, optical access networks and chip-to-chip communications in a super-computer [1, 2]. Among various MWLs [3–6], the distributed-feedback (DFB) laser is one of the most promising candidates to realize single-longitudinal-mode operation with a precise spectral control. Conventionally, realizations of a stable and multi-wavelength lasing of a DFB MWL array have technical challenges: first of all, multi-wavelength lasing requires that each laser in the array must have a different Bragg wavelength, which means that the period of the grating in each laser should be different [7]; secondly, a quarter-wave phase shift [8] or a chirped grating with an equivalent quarter-wave phase shift distributed over a region [9, 10] should be introduced in the middle of a uniform grating to ensure single-longitudinal-mode operation and reduce mode degeneracy caused by the poor mode-selectivity and the spatial hole burning (SHB). Both technical requirements, which need a precise control of each grating line in a nanometer scale, cause the fabrication process very complicated, time-consuming and costly since it requires techniques such as multiple holographic exposures or electron-beam lithography (EBL). Although many solutions have been proposed, such as the use of bent waveguides and phase masks [11, 12], they are usually not suitable for practical mass production due to the unreliable performance. Therefore, a simple approach suitable for mass production with high performance at a low cost is urgently required.

Recently, we have proposed an equivalent chirp technology (ECT) to realize an equivalent grating structure based on nonuniformly sampling a uniform Bragg grating [13]. The use of the ECT in the design of a DFB MWL array was studied theoretically [13]. For a DFB laser based on the ECT, its wavelength is determined by not only the Bragg grating period but also the sampling function. In addition, by properly controlling the sampling function, an advanced grating structure, such as a phase-shifted grating or a chirped grating profile, can be realized. Therefore, with the conventional low-cost holography technology and a pre-designed sampling mask to define the sampling function for each laser, a DFB MWL array can be fabricated by writing a homogeneous grating on the entire wafer. The significance of the ECT is its capability of using a standard fabrication process in a commercial foundry and reducing the fabrication cost dramatically while maintaining the same laser performance. In addition, the ECT enables the implementation of a grating with a complicated profile, such as a chirped profile instead of a phase-shifted profile inside the cavity, which would make the power of the lasing wavelength distributed more uniformly over a large area, and consequently decrease the power density inside the cavity, ease the heat effect and potentially enhance the output power. Although a single ECT-based DFB laser or an ECT-based MWL array with an equivalent phase-shifted grating has been experimentally demonstrated [14–16], no ECT-based MWL array with a more complicated grating profile has been fabricated and demonstrated. In this paper, for the first time, to the best of our knowledge, an ECT-based DFB MWL array with an equivalent chirped grating profile is designed, fabricated, and tested. The laser array exhibits good single-longitudinal mode operation and multiple-wavelength lasing performance, which shows the ECT is an effective solution for monolithic integration of a MWL arrays that are suitable for low cost mass production.

2. Principle

Based on the ECT, an advanced grating structure, such as a chirped and phase-shifted grating, can be implemented by nonuniformly sampling a uniform Bragg grating. The sampled grating can be considered as a combination of many subgratings. Each subgrating has a different Bragg wavelength and a grating profile, which can be modified by changing the sampling function. Mathematically, the index modulation change $\Delta n(z)$ of an ECT-based Bragg grating can be expressed as

$$\Delta n(z)=\frac{1}{2}s(z)\exp\left(j\frac{2\pi z}{\Lambda}\right)+c.c=\frac{1}{2}s_0\left[z-\frac{\varphi(z)P}{2\pi}\right]\exp\left(j\frac{2\pi z}{\Lambda}\right)+c.c \tag{1}$$

where Λ is the grating period, $s(z)$ is a nonuniform sampling function, $s_0(z)$ is a periodic sampling function, which is a square wave with a period of P, and $\varphi(z)$ is the chirp profile which can be achieved equivalently by the nonuniform sampling. Applying Fourier series expansion to $s_0(z)$, Eq. (1) can be rewritten as

$$\Delta n(z)=\sum_m \frac{1}{2}F_m\exp\left[-jm\varphi(z)+j\frac{2\pi z}{\Lambda_m}\right]+c.c \tag{2}$$

where F_m is the mth-order Fourier coefficient, and $\Lambda_m=\Lambda P/(m\Lambda+P)\approx\Lambda-m\Lambda^2/P$. As can be seen from Eq. (2), an ECT-based nonuniformly sampled Bragg grating can be considered as a superposition of multiple subgratings, with each subgrating having a uniform grating period Λ_m and a chirp profile $m\varphi(z)$. By properly choosing P, we can make the spectral response of only one subgrating, say −1st subgrating, fall into the gain spectrum of the semiconductor material, while the spectral responses of all the other subgratings are located outside the gain spectrum. Therefore, only the wavelength within the −1st subgrating is possible to lase, and for the −1st subgrating, an equivalent chirp profile $\varphi(z)$ is achieved based on the ECT.

In a conventional DFB laser, to ensure a single-longitudinal-mode operation, a quarter-wave phase shift or a chirped grating profile with an equivalent quarter-wave phase shift distributed over a center region should be introduced to produce a narrow transmission band in the imbedded grating. Assume that a linear chirp profile introduced is expressed as

$$\varphi(z)=\begin{cases}0, & -L/2\le z<-D/2\\ \dfrac{\pi}{D}\times\left(z+\dfrac{D}{2}\right), & -D/2\le z<D/2\\ \pi, & D/2\le z\le L/2\end{cases} \tag{3}$$

where L is the length of the grating and D is a value to define the length of the linear chirp profile region. Then, based on Eq. (1), we can have the sampling function of the grating in an ECT-based DFB laser. Since $\varphi(z)$ is a nonlinear function, the nonuniform sampling period P_s also changes nonlinearly over the whole grating, which is given by

$$P_s = \begin{cases} P, & -L/2 \le z < -D/2 \\ \dfrac{P}{1 - P/2D}, & -D/2 \le z < D/2 \\ P, & D/2 \le z \le L/2 \end{cases} \quad (4)$$

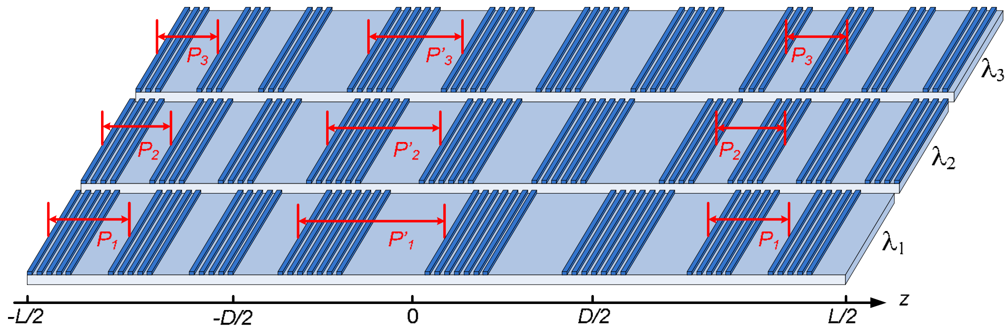

Fig. 1. Schematic of the grating structures of an MWL array based on the ECT.

Figure 1 shows the schematic of the grating structure of an ECT-based laser array.

From Eq. (2), we can also see that the lasing wavelength of an ECT-based DFB laser can be given by

$$\lambda_L \approx 2n_{eff}\Lambda_{-1} = 2n_{eff}\frac{P\Lambda}{P-\Lambda} \quad (5)$$

which shows that the lasing wavelength is determined by not only the grating period, but also the sampling period. Therefore, we can design a DFB laser with different lasing wavelength by choosing a different sampling period, while keeping the grating period unchanged, which simplifies the fabrication significantly. Therefore, the ECT makes it possible to fabricate a DFB MWL array on a wafer with a homogeneous grating and a desired chirp profile. Both the lasing wavelength and the chirp profile can be designed by controlling the sampling functions in a micrometer scale rather than the grating period in a nanometer scale.

3. Fabrication and experimental results

A DFB MWL array is fabricated in the Canadian Photonics Fabrication Centre (CPFC), a commercial InP foundry in Canada. Two-step MOCVD is employed to grow a standard 1.55 μm InGaAsP/InP laser structure on a 3-inch n-InP substrate. An InP buffer layer, a lower optical confinement layer, a multiple quantum-well (MQW) active structure and a grating layer are successively grown during the first epitaxy. Then, a thin layer of oxide is deposited on the wafer. Standard photolithography transfers the pre-designed sampling mask onto the wafer where the desired wavelengths and sampling functions are defined by the sampled grating areas. The values of the sampling periods on the pre-designed mask are calculated based on Eq. (5) for given lasing wavelengths. The sampled gratings are then formed by a conventional holographic exposure followed by wet etching. Then, the wafer is grown once more to form an upper optical confinement layer. The wafer is then further processed into ridge waveguide (RWG) lasers with a ridge width of 2 μm. The wafer is cleaved, and the cavity length of each laser is 400 μm. Both facets of the lasers are as cleaved. The measured grating period is 232 nm, and the estimated effective index is around 3.19. The sampling period over the laser array is about several μm.

Figure 2 shows the microscopic image of the fabricated sampled grating before the MOCVD overgrowth. Figure 3 shows the cross section image of one fabricated DFB laser after the MOCVD overgrowth.

#192100 - $15.00 USD Received 11 Jun 2013; revised 1 Aug 2013; accepted 1 Aug 2013; published 16 Aug 2013

Figure 4 shows the spectrum of one laser in the fabricated ECT-based MWL array biased at 20 mA. The spectrum is centered at 1565 nm with a 3-dB width of about 20 nm.

The power-current (P-I) curves and threshold currents at different ambient temperature of the laser are then measured, as shown in Fig. 5. The slope efficiency is 0.444W/A and the threshold current is 24 mA when the temperature is at 20°C. With the increase of the temperature, the slope efficiency decreases but can also reach a value up to 0.252W/A even at a temperature of 90°C.

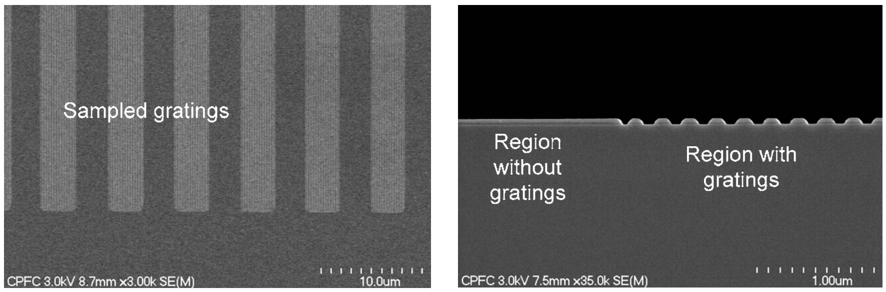

(a) (b)

Fig. 2. (a) Top view of the etched sampled gratings, and (b) cross-section image of the sampled gratings (before the MOCVD overgrowth).

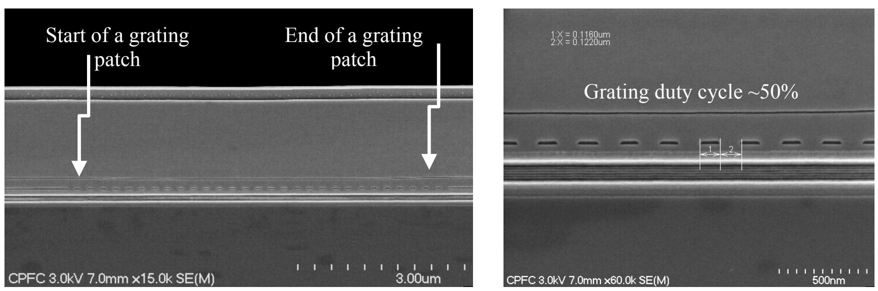

(a) (b)

Fig. 3. (a) Image of the cross section of an ECT-based DFB laser; (b) zoom-in view of the cross section (after the MOCVD overgrowth).

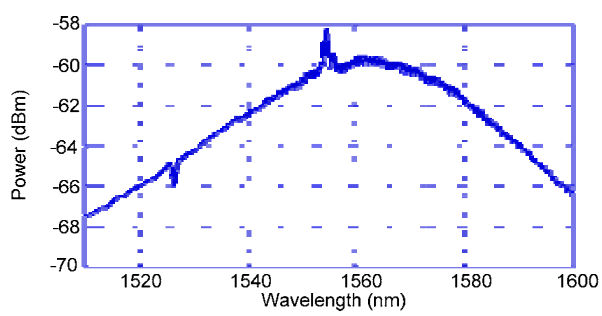

Fig. 4. Measured spectrum of one laser in the fabricated ECT-based MWL array.

Two laser arrays are then selected to measure their lasing spectra. Figures 6(a) and 6(b) shows the spectra of an MWL array with four and six wavelengths, respectively. The average wavelength spacing for the two laser arrays in Figs. 6(a) and 6(b) are about 2 nm and 1 nm, respectively. For the first array, the average measured single-mode suppression ratio (SMSR) and the maximum SMSR are 30 dB and 38 dB, respectively, which exhibits good single-longitudinal mode operation performance. For the second array, the measured average SMSR

#192100 - $15.00 USD Received 11 Jun 2013; revised 1 Aug 2013; accepted 1 Aug 2013; published 16 Aug 2013

and the maximum SMSR are 35 dB and 40 dB, respectively. The relatively small SMSR is due to the fact that effective index modulation of each subgrating of the sampled grating is weaker than a uniform grating [17], and weaker index modulation would cause poorer mode selectivity. To increase the SMSR, the index modulation of the original uniform grating must be enhanced. The laser facets may also be coated to suppress the side modes.

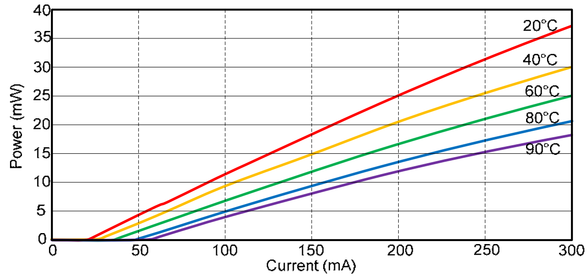

Fig. 5. The measured P-I curve under different ambient temperatures.

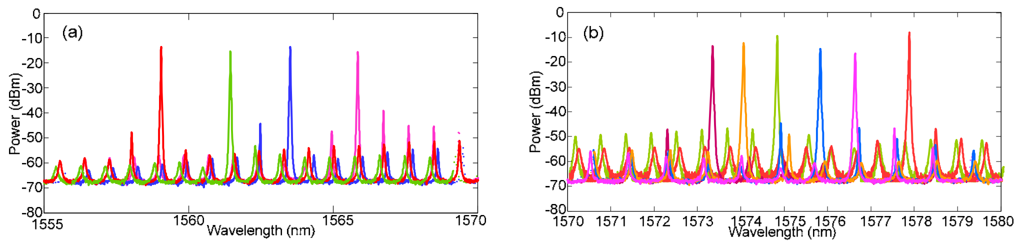

Fig. 6. Measured optical spectrum of two MWL arrays with different wavelength spacing.

4. Discussion and conclusion

Note that the ECT is applicable to the design of laser sources operating at any wavelength regimes, determined by the gain spectrum of the gain material and the pitch of the sampled grating. For example, a DFB laser based on GaAs designed based on the ECT can cover a wavelengt range from 780 to 850 nm.

In summary, we have reported the design, fabrication and testing of ECT-based DFB MWL arrays with a chirped grating profile. Two ECT-based DFB MWL arrays with multiwavelength lasing having four and six wavelengths were demonstrated. For each wavelength, single-longitudinal mode operation was ensured. Good linearity of the power-current curve was also achieved. The key significance of the work is the use of the ECT, which enables the fabrication of laser arrays with a single conventional holographic exposure. The experimental results showed that the ECT could be an effective solution for the production of DFB laser arrays at low cost. Based on the ECT, more wavelengths with flexible wavelength spacing could also be achieved, and such multi-wavelength sources could find applications in microwave photonic systems for microwave signal processing. Multiwavelength laser sources with a large number of wavelengths can also find applications for true time delay beamforming [18].

Acknowledgments

This work was supported in part by the Natural Sciences and Engineering Research Council of Canada (NSERC) through the Strategic Grant Project program and CMC Microsystems.